the initial activity per unit mass of tumor (C_0) reported to produce 0.9 cure probability at the optimal size was used. Cure probability with no magnetic field present is compared to the result when a 10-Tesla magnetic field is applied.

The two curves shown in Figure 1 clearly illustrate that the application of the magnetic field extends the range of potentially curable tumors significantly. Submillimeter lesions, however, are predicted to be incurable. What is not shown is the up to 80% reduction in absorbed radiation dose to adjacent normal tissues from radiopharmaceutical accumulated in the tumor, which in some applications, can limit the injected amount of radionuclide and therefore the effectiveness of the treatment. Hence, the use of magnetic confinement allows for more efficient utilization of emitted beta particles. The length of time a patient must spend in the magnet basically depends on the physical half-life of the radionuclide and localization time of the radiopharmaceutical. Therefore, ^{90}Y may not be the optimal choice as a MERiT radionuclide, instead a beta-emitter with a shorter half-life such as ^{188}Re might be more appropriate, if rapid localization is achieved.

Undeniably, the use of a multiradionuclide regimen is presently the most feasible way to target treatment to both primary and metastatic tumors. Future advancements in the fields of magnet design and radiopharmaceuticals may allow MERiT to become a useful technique in the treatment of cancer. Perhaps MERiT could be utilized in tandem with multiradionuclide approaches to maximize therapeutic effectiveness for a wider range of tumor sizes compared to the conventional approach. Regardless, discussion of the limitations of curability due to tumor size should include a mention of MERiT, even if it is currently impractical and expensive.

REFERENCES

1. O'Donoghue JA, Bardiès M, Wheldon TE. Relationships between tumor size and curability for uniformly targeted therapy with beta-emitting radionuclides. *J Nucl Med* 1995;36:1902–1909.
2. Wheldon TE, O'Donoghue JA, Barret A, Michalowski AS. The curability of tumors of differing size by targeted radiotherapy using ^{131}I of ^{90}Y. *Radiother Oncol* 1991;21:91–99.
3. Raylman RR, Wahl RL. Magnetically enhanced radionuclide therapy. *J Nucl Med* 1994;35:157–163.

Raymond R. Raylman
Richard L. Wahl
University of Michigan
Ann Arbor, Michigan

Angular Sampling Necessary for Clinical SPECT

TO THE EDITOR: The recent article by Rosenthal et al. (*1*) provides a useful overview of quantitative SPECT, which undoubtedly will be used as a valuable educational reference. The article includes description and discussion of several important basic aspects of SPECT, including essential practical considerations. One important consideration is the choice of the number of projection angles for data acquisition which is often poorly understood. Unfortunately, the description of angular sampling provided by Rosenthal et al. (*1*) is in some respects ambiguous, such that readers are likely to derive an incorrect conclusion as to the required number of detector positions for SPECT acquisition. I hope that the following description may clarify the ambiguities related to angular sampling requirements and provide an intuitive basis for practical use.

As pointed out by Rosenthal et al. (*1*), the matrix size should be chosen so that the pixel size is less than half the resolution expected (essentially ensuring that the sampling theorem is satisfied and that the maximum spatial frequency in a study is preserved). It is then reasonable to suggest that the same sampling distance be preserved in the angular direction for any point in the reconstructed matrix. Consider Figure 1, which illustrates the gamma camera's position for two adjacent angular projections. The sampling distance can be considered as the arc (A in Fig. 1) subtended by

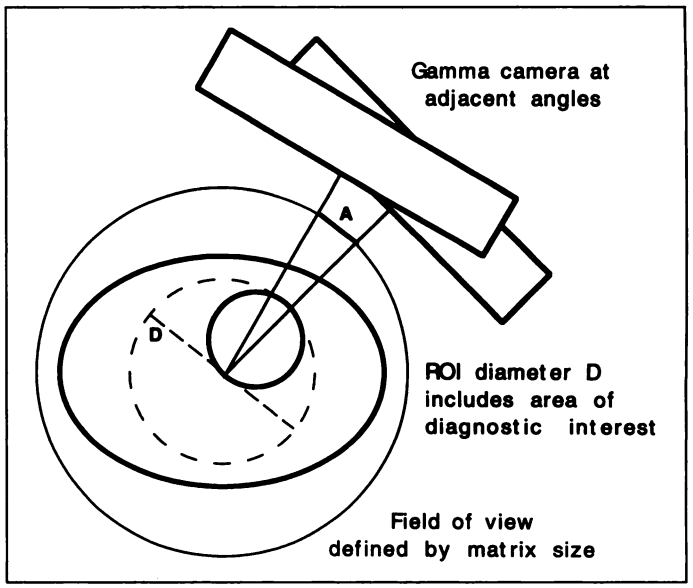

FIGURE 1. SPECT acquisition for a study of the thorax. Necessary angular sampling for complete reconstructed field of view requires that arc A be less than $\delta x/2$ (where δx is the resolution distance). For a cardiac study, however, it is sufficient for angular sampling to be satisfied on the circumference of the ROI diameter D, which encloses the region of diagnostic interest.

the angle between adjacent projections at any radius. The maximum arc is at the edge of the matrix; so if this arc is less than half the resolution distance, the complete matrix will be sufficiently well sampled. This would suggest an equation for the necessary number of separate angles over 360 degrees (N) to be:

$$N = \pi D/(\delta x/2)$$

using identical notation to Rosenthal et al's. article, where D is the field size and δx is the resolution distance. Note that the resultant equation is different to that provided by Rosenthal et al. (*1*) by a factor of two. N refers to the number of individual projections or detector positions over 360° rather than the number of projection angles over 180°. Some authors define the number of projection angles as that required over 180°, on the basis that opposite views can be considered "at the same angle." Of course, in the absence of attenuation, as for CT scanning, sampling over 180° is sufficient with opposite views being identical. This may contribute to the ambiguity.

Several authors have related N directly to the matrix size with particular concern for reconstruction streak artifacts that occur with poor angular sampling (*2–5*). In the case where the whole field is sampled at exactly $\delta x/2$, $D/(\delta x/2)$ corresponds to the matrix size (M) and $N = \pi M/2$ over 180°, approximated by some to 1.5 M. These formulae have fairly wide acceptance (*6*) but tend to suggest a higher number of angles than is used in clinical practice. It is reasonable to suggest that sampling be sufficient over all parts of the images that have diagnostic information and thus it is possible to relax the requirement that the complete matrix area be sufficiently sampled. Rosenthal et al. (*1*) recognize this and point out that D can be considered the "diameter of a circle enclosing the region of interest." The diameter (D), however, must refer to a circle centered on the axis of rotation. This is illustrated in Figure 1 for a cardiac study, in which D clearly exceeds the minimum diameter circle which could enclose the cardiac region.

It is useful to consider typical clinical examples to illustrate the correct choice of number of angles:

1. For cardiac studies acquired over 180° using a camera of 400-mm field size, reconstructed resolution is typically around 16 mm. The linear sampling therefore requires a pixel size of less than 8 mm corresponding to a matrix size typically 64 × 64. The centre of rotation is typically towards the posterior wall of the heart and the heart diameter is of the order of 100 mm. Use of the revised equation

to estimate the number of projections required gives N = π.200/(16/2), approximately 78 projections over 360° or half that number over 180°. This suggests that the number of projections should be greater than the 32 commonly used, although use of 64 projections over 180° is overkill (48 angles might be considered ideal). Note that the number of angles has no direct relationship to the matrix size chosen or zoom factor used for either acquisition or reconstruction, contrary to some authors' discussions (*2–5*).

2. For brain studies, the region of diagnostic interest tends to be located centrally. Therefore, in this case, the value for D does correspond to the dimension of the brain, typically 160 mm. Reconstructed resolution for brain studies is significantly better than that for cardiac studies and can be as low as 8 mm. Therefore, with a camera of 400-mm field size, a 128 × 128 matrix size is required to preserve resolution. The number of angles required is N = π.160/(8/2), approximately 125 angles over 360°. This is consistent with common practice. Note again that this is independent of the matrix size chosen; a zoomed acquisition using a smaller matrix size still requires the same number of projection angles.

The choice of angular sampling is frequently misunderstood and rarely appreciated. The discussion and illustration presented here, although intuitive, appears consistent with more rigorous descriptions and should assist readers in deciding what protocols are appropriate for any applications.

REFERENCES

1. Rosenthal MS, Cullom J, Hawkins W, Moore SC, Tsui BMW, Yester M. Quantitative SPECT imaging: a review and recommendations by the focus committee of the Society of Nuclear Medicine Computer and Instrumentation Council. *J Nucl Med* 1995;36:1489–1513.
2. Bracewell RN, Riddle AC. Inversion of fan-beam scans in radio astronomy. *Astrophys J* 1967;150:427.
3. Snyder DL, Cox JR. An overview of reconstruction tomography and limitations imposed by a finite number of projections. In: *Reconstruction tomography in diagnostic radiology and nuclear medicine*. University Park Press; 1977:3.
4. Huesman RH. The effects of a finite number of projection angles and finite lateral sampling of projections on the propogation of statisical errors in transverse section reconstruction. *Phys Med Biol* 1977;22:511–521.
5. Larsson SA. Gamma camera emission tomography. *Acta Radiol* 1980;363(suppl):21–22.
6. Bailey DL, Parker JA. Single-photon emission computerized tomography. In: Murray IPC, Ell PJ, eds. *Nuclear medicine in clinical diagnosis and treatment*, vol. 2. Edinburgh: Churchill Livingstone; 1994:1315–1326.

Brian Hutton
Westmead Hospital
Sydney, Australia

Carbon-14-Urea Breath Test: A Cautionary Note

TO THE EDITOR: We currently perform about 75 ^{14}C-urea breath tests annually based on the method of Marshall and Surveyor (*1*). Our experience with this test has highlighted the significance of fasting before the study. The paper by Marshall et al. (*2*) discusses the different results obtained between patients who fasted and those who ate a test meal. Our concern relates to clinicians using a reference range based on fasting patients, who may not be rigorous in their application of this fasting criterion.

Although our procedure for ^{14}C-urea breath testing involves informing the patient to fast (at least 6 hr) and confirming that the patient did indeed fast before the test commences, there are instances when this routine is not followed. On two occasions, patients started the test without fasting. These patients underwent a repeat study after fasting; the results from the second study are shown in Table 1.

We measure the $^{14}CO_2$ at 5-min intervals for 30 min and calculate the peak value after 10 min as: % dose/mmole CO_2 × body weight. We also measure the area under the curve after 10 min.

Both patients would have had equivocal or normal results because the test values were affected by the presence of food in their stomachs. Their fasting values, however, were both positive for *Helicobacter pylori*. Unfortunately, there were no other follow-up tests performed to verify our results and, hence, the presence of *H. pylori*. The significant elevation of the fasting values warrants careful examination of the fasting state of each patient.

TABLE 1
Results for Carbon-14-Urea Breath Test before and after Fasting

	Nonfasting		Fasting	
Patient no.	Peak value	Area under curve	Peak	Area under curve
1	1.26	20.4	3.29	55.2
2	0.84	13.8	2.5	42.0

Our fasting reference ranges were: <0.5 normal; 0.5–1.5 equivocal: >1.5 positive for peak value; and 0–16 normal; 16–25 equivocal: >25 positive for the area under curve.

REFERENCES

1. Marshall BJ, Surveyor I. Carbon-14-urea breath test for the diagnosis of *Campylobacter pylori* associated gastritis. *J Nucl Med* 1988;29:11–16.
2. Marshall BJ, et al. A 20-minute breath test for *Helicobacter pylori*. *Am J Gastroenterol* 1991;86:4:438–445.

T. Warwick
Sir Charles Gairdner Hospital
Nedlands, Western Australia

Which Is Better for Inferior Wall Evaluation: A Full or Empty Stomach?

TO THE EDITOR: Technetium-99m-tetrofosmin, recently introduced as an agent for myocardial perfusion imaging, is excreted mainly by the biliary system (*1*). High intestinal activity may be seen in a one-day imaging protocol. This intestinal activity may create a major problem in the visual interpretation of the inferior myocardial wall, especially in the rest imaging.

In the study of Braat et al. (*2*), the inferior wall of myocardium was considered ischemic in three patients by at least two of the three different observers in the one-day protocol while in the two-day protocol, the same region was defined as scar tissue by the observers. The explanation for this discrepancy was proposed to be scatter from the abdominal and hepatic background to the inferior wall of the myocardium.

In our early studies with ^{99m}Tc-tetrofosmin, we told patients to have their normal meal 45–60 min before rest imaging. Imaging starts 20–30 min after injection and patients are advised to drink 200–300 cc water

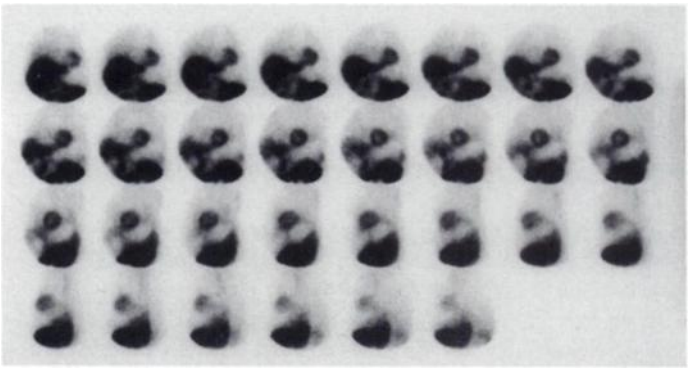

FIGURE 1. Raw data of rest myocardial SPECT image 20 min after an intravenous dose of 20 mCi of ^{99m}Tc-tetrofosmin. The patient was allowed to have his daily meal 1 hr before injection. Filled stomach appears as a photopenic area between myocardium and intestines in the frames.